Flow Structure Development Due to Water Injection into the Annulus of Heavy Oil Pipe Flow

تطور هياكل السريان نتيجة حقن الماء فى المجري الحلقى حول سريان الزيت الثقيل فى أنبوب

by

Ahmed L. Sakr, G.I. Sultan, M. G. S. Mousa, and M. M. Tolba,

Mechanical Engineering Dept., Faculty of Engineering, Mansoura University

Abstract

This work investigates the flow structure development due to injecting water into the annulus of heavy oil pipe flow. Numerical simulation of the axisymmetric core-annular turbulent flow is carried out using the standard k–ω model. The flow field and flow characteristics are investigated using FLUENT 6.3.26. The core-annular flow of heavy oils-water in 15.24 cm diameter pipe, with three core diameters is considered. The influence of flow parameters upon the development of axial and radial velocity, turbulent kinetic energy, turbulence intensity, and strain rate profiles are investigated.

Results show that the flow development depends on the core to outer diameters ratio, oil viscosity, flow velocity, and water loading ratio. As oil's viscosity increases, the flow structure develops faster towards fully-developed one. Fully-developed velocity profiles show uniform distribution in oil's core, while all velocity changes occur in water flowing in pipe annulus. The flow in the core region seems to be as rigid body carried by annular water flow. It has been demonstrated that major changes in flow structure occur at the oil-water interface.

ملخص البحث

تقدم هذه الورقة دراسة عددية لتطور هياكل السريان نتيجة حقن الماء حول الزيوت الثقيلة فى خطوط الأنابيب الناقلة بحيث يسري الماء حلقياً فاصلا الزيت الثقيل عن السطح الداخلى للأنبوب، وذلك بغرض تخفيض المفاقيد الاحتكاكية. تم استخدم برنامج ديناميكا الموائع الحسابية المعروف Fluent 6.3.16 لحل معادلات الحركة للسريان المضطرب للزيوت الثقيلة والماء فى أنبوب ذي قطر ٦ بوصة. وقد تم استخدام أنواع عديدة من الزيوت الثقيلة تراوحت لزوجتها من ٣٠ الى ١٨٠٠٠ سنتى بواز. كما تم دراسة العوامل المختلفة المؤثرة على تطور التوزيع المقطعى للسرعة، وطاقة الاضطراب.

توضح النتائج ان لزوجة الزيت الثقيل، معدل السريان، نسبة قطر الزيت فى القلب الى قطر الأنبوب، ونسبة كمية الماء إلى كمية الماء والزيت، وسرعة الماء الى سرعة الزيت عند الدخول لها تأثير كبير على تطور هيكل السريان من لحظة حقن الماء حتى الوصول إلى التطور الكامل، وأنه كلما ارتفعت لزوجة الزيت الثقيل كلما أصبح التطور اسرع. كما توضح النتائج أن توزيع السرعة على أي مقطع كامل التطور أظهر سرعة ثابتة للزيت الثقيل فى قلب الانبوب بينما سرعة الماء فى المقطع الحلقي تتغير من صفر على السطح الى قيمة عظمى عند السطح الفاصل بين الماء والزيت، وأصبح الشكل العام للسريان مماثلا لسريان الزيت الثقيل كجسم صلب فى قلب الانبوب يحمله سريان الماء الحلقى المحيط به.

Accepted February 28, 2013

1. Introduction

The progressive increase of oil demand coupled with the depletion of light crude oils has led to rapid development of the large world resources of heavy oils and bitumen. Conserved estimates show that heavy oil reserves are more than six trillion barrels throughout the world. The main problem of heavy oils production is the difficulty of transportation, due to the immense power requirement. Water lubrication of heavy oils and bitumen is an effective method for oil transportation in pipelines. Water is injected into the wall to encapsulate oil flows in the core region by annular water film along the pipe wall. This reduces drastically the pumping power and its cost of transportation of bitumen and heavy oil. Such common flow pattern of two-fluid pipe flow of immiscible liquids is well-known as core-annular flow "CAF". Strazza et al (2011) stated that the pressure drop of oil-water core-annular flow is comparable to that of water flowing alone in pipeline even for extra heavy oils. Reviews on core-annular oil-water flow are found in Joseph et al. (1997), Xu (2007) and Ghosh et al. (2009). They surveyed studies on different aspects of the phenomenon covering models for levitation, determination of pressure drop, classification of flow types, and empirical correlations.

Clark and Shapiro (1949) presented the earliest works on core-annular flow in pipeline. Since that time numerous studies have been performed. Charles et al.(1961) presented the earliest work to discuss CAF scientifically. Oliemans (1986) analyzed the feasibility of CAF as function of oil viscosity, showing that the higher the oil viscosity the easier is the formation of this flow regime. Bannwart (2001), Ooms and Poesio (2003), and Ooms et al. (2007) focused their attention on the levitation mechanism, which allows the oil to flow surrounded by a film of water. Ooms et al. (1984) studied the core-annular flow of highly viscous oil and water in two horizontal pipelines. Oliemans et al. (1987) studied experimentally the core-annular flow of oil (μ=3000 cP) and water in 5 cm diameter horizontal pipe of 16 m length.

Miesen et al. (1993) studied core-annular flow of fuel oil (μ=3900 - 25000 cP) and crude oil (μ=7000 - 27000 cP) in two horizontal test-loops; 5 cm diameter 12 m long, and 20 cm diameter 1000 m long pipes. Bai et al. (1992) performed experiments with motor oil (μ=600 cP) using 0.95 cm diameter pipe in vertical up/down flow. Bensakhria et al. (2004) studied the flow of heavy oil (μ=4740 cP) and water in pipeline 2.5 cm diameter and 12 m length. Sotgia et al. (2008) studied experimentally oil water flow in horizontal pipes using mineral oil and water of viscosity ratio about 900. The results of all these studies show that the injection of small amounts of water into the annulus of heavy oil pipe flow causes significant pressure loss reduction.

Bannwart (2001) discussed several aspects of core-annular flow modeling in the light of experimental data. The results show that the largest oil flow rate requires lesser amounts of water for the minimum pressure gradient. Grassi et al. (2008) carried out study to validate the models developed and summarized by Brauner and

Ullmann (2002) for the prediction of pressure drops in core-annular flow. Pressure drop predictions show satisfactory agreement with the experimental results. Rodriguez et al. (2009) proposed pressure-loss prediction model for core-annular flow. The model shows excellent agreement with their experimental data and data from the literature.

Limited number of numerical studies to model the core-annular flow of heavy oil and water are found. Huang et al. (1994) used the standard k–ε turbulence model to study turbulent core-annular flow. Satisfactory agreement between model predictions and experimental and field data from all sources was found.

Rovinsky et al. (1997) carried out prediction of the flow characteristics of eccentric, laminar annular flow. They expressed velocity profiles, pressure drop reduction factor and power saving factor as function of viscosity ratio of two phases and reported that power saving factor increases with increase of viscosity ratio.

Ko et al. (2002) extended the numerical simulation of axisymmetric laminar core–annular flow to turbulent case by adopting the shear stress transport (SST) k–ω model proposed by Menter (1994). Torres-Monzon (2006) developed 2D model for oil-water flow in horizontal and near horizontal pipes. The model for fully-developed, turbulent-turbulent oil-water flow was presented. It was based on numerical solution of the basic governing equations using finite-volume method. The pressure gradient calculated from turbulent code satisfied Blasius formula in the turbulent core–annular flow with a rigid core.

The aforementioned discussion reveals that there is limited number of numerical studies concerning the core-annular flows of heavy oils and water. Many aspects need to be clarified such as flow structure and the influence of different parameters on pressure reduction. This work investigates the flow structure development due to injecting water into the annulus of heavy oil pipe flow. Numerical simulation of the axisymmetric core-annular turbulent flow is carried out using the standard k–ω model. The flow field and flow characteristics are investigated using the Computational Fluid Dynamics (CFD) FLUENT 6.3.26 package. The influence of flow parameters upon the development of axial and radial velocity, turbulent kinetic energy, turbulence intensity, and strain rate profiles are investigated.

2. ***Problem Description***

Numerical simulation of the core-annular flow in a pipe is carried out using the standard k–ω model. The flow is assumed to be turbulent and axisymmetric. The geometry of the computational model of the core-annular pipe flow is developed using GAMBIT. It consists of a 6 inches diameter (D_o=15.24 cm) pipe of 920 cm length, and an inner pipe of variable diameter (D_i=14.6 cm, 14.0 cm, and 12.7 cm) and 100 cm length. These two pipes are fixed in concentric manner such that the inner pipe extends 20 cm inside the outer pipe forming an annulus of 20 cm length, as shown in Figure (1).

Heavy oil flows through the inner pipe forming the core flow, while water is allowed to flow through the annulus between the outer pipe and the oil core. Figure (2) presents the flow field geometry and coordinate system computational domain. For axisymmetric 2D flow, the centerline of the pipe is taken as the axis of symmetry, and half of the flow configuration is taken as the computational domain. Three flow configurations of core to pipe diameters ratio α ($\alpha = D_c/D_o$) are 0.96, 0.92, and 0.83 respectively. The flow is assumed to be axial, and *2D* axisymmetric. Heavy oil is confined in the core region with diameter "D_c" and water is flowing in the annulus region between oil in the core and the pipe wall of diameter "D_o". The two fluids are immiscible, and the interface between the heavy oil and water is smooth and perfect, and no slip between the two phases. Water flow in the annulus is assumed to be turbulent.

3. *Mathematical Formulation*

Flow predictions are carried out by solving the Navier-Stokes equations for turbulent flow of Newtonian fluid through the pipe using the well-known CFD package Fluent 6.3.26. The turbulent model considered in this work is the Standard *k-ω* turbulence model. The model adopted is an axisymmetric *2ddp* (*2D*, double precision Fluent solver) turbulent flow one. The model uses the continuity equation and Reynolds-Averaged Navier-Stokes (RANS) equations as;

$$\frac{\partial \rho}{\partial t} + \frac{\partial}{\partial x_i}\left(\rho \overline{u_i}\right) = 0 \qquad (1)$$

$$\frac{\partial U_i}{\partial t} + U_j . \frac{\partial U_i}{\partial x_j} = -\frac{1}{\rho} . \frac{\partial p}{\partial x_i} + \frac{1}{\rho} . \frac{\partial}{\partial x_j}\left(\mu . \frac{\partial U_i}{\partial x_j} - \rho \overline{u_i' u_j'} \right) \qquad (2)$$

where the Reynolds stresses $\rho.\overline{u_i'.u_j'}$ are the normal and shear stress terms. These equations must be coupled with a turbulence model to correlate Reynolds stresses with main flow parameters as,

$$\rho \overline{u_i' u_j'} = \mu_t \frac{\partial U_i}{\partial x_j} \qquad (3)$$

The standard *k-ω* model relates the eddy viscosity to the turbulent kinetic energy (*k*) and the specific dissipation rate (*ω*) of turbulence.

$$\mu_t = \rho . C_\omega . \frac{k}{\omega} \qquad (4)$$

where C_ω is constant.

The transport equations of (*k*) and (*ω*) are to be solved with Reynolds-Averaged Navier-Stokes to predict turbulent flow fields [Wilcox (1998)]. The two transport equations are given as

$$\frac{\partial}{\partial t}(\rho k) + \frac{\partial}{\partial x_i}(\rho k u_i) = \frac{\partial}{\partial x_j}\left(\Gamma_k \frac{\partial k}{\partial x_j} \right) + G_k - Y_k + S_k \qquad (5)$$

and

$$\frac{\partial}{\partial t}(\rho \omega) + \frac{\partial}{\partial x_i}(\rho \omega u_i) = \frac{\partial}{\partial x_j}\left(\Gamma_\omega . \frac{\partial \omega}{\partial x_j} \right) + G_\omega - Y_\omega + S_\omega \qquad (6)$$

where G_k and G_ω are the generation of k and ω due to the mean velocity gradients respectively, Γ_k and Γ_ω are the effective diffusivity of k and ω, respectively, Y_k and Y_ω are the dissipation of k and ω due to turbulence, and S_k and S_ω are user-defined source terms.

Problem Boundary Conditions

For the physical model of the 2D axisymmetric core-annular pipe flow shown in Figure (2), the cylindrical coordinate system considered where x_i and the mean averaged velocity components will be written as

$$x_1 = r, \quad \text{and} \quad x_3 = z, \tag{7}$$

$$U_1 = U_r = v, \text{ and } U_3 = U_z = u \tag{8}$$

At the inner surfaces walls of the outer and inner pipes, lines BB1, and AC1, and the outer surface wall of inner pipe CC1, the velocity components are zeros

$$v = u = 0 \tag{9}$$

At the axis of symmetry, OO1, the velocity gradients are zero

$$\frac{\partial u}{\partial z} = \frac{\partial v}{\partial z} = \frac{\partial k}{\partial z} = \frac{\partial \omega}{\partial z} = 0 \tag{10}$$

At the inlet cross section of the core "face OA", the heavy oil flows in with uniform velocity equals U_o, and the annulus "face CB", water flows in with uniform velocity equals U_w. At the exit section of the pipe "face O1B1", exit pressure is uniform and equals the atmospheric pressure. For the k-ω model, the values of k and ω on the solid walls are taken as $k = 0$, and ω is set using Wilcox's roughness model [Wilcox, (1998)]. At the inlet the turbulence intensity "I" and turbulent viscosity are specified, and the turbulent kinetic energy k is calculated from:

$$k = \frac{3}{2}.I^2.U_{in}^2 \tag{11}$$

4. *Numerical Technique and Procedure*

The governing equations for the turbulent flow are solved numerically to predict the flow field and flow parameters. Numerical solution is carried out by discretizing the partial differential equations using the finite volume technique. The values of the dependent variables are considered at finite number of locations called the grid points. The entire flow domain is divided into control-volumes with grids at their geometric centers and all the variables defined at those grid points. From the differential equations governing the chosen variables, the algebraic equations are derived for the grid-point values of the variables. Therefore, the method includes the tasks of formulating algebraic equation for these unknowns and prescribing an algorithm for solving these equations.

Considering flow configurations of core to pipe diameters ratio α=0.83, to mesh the core region, a mesh on the rectangular face OO1AA1 is created with 2000 divisions in the axial direction and 40 divisions in the radial direction. For the annular region, meshing the rectangular face BB1CA1 is created with 1840 divisions in the axial direction and 20 divisions in the radial direction. Mesh is generated by meshing the four edges first, and then the face is done. The desired grid spacing is specified through the edge mesh.

To resolve the much higher gradient near the wall for the turbulent flow, smaller grid spacing near the wall is used by employing grid stretching. Smaller grid spacing near the oil-water interface wall is also used. For each vertical edge, the division length next to the wall is specified to be 0.001 and the total number of divisions to be 40 in the core region and 20 in the annulus. Convergence criterion of $1x10^{-5}$ was

chosen for r and z velocity components as well as the continuity equation, turbulent energy k, and turbulent dissipation frequency ω. For the model developed uses the first order upwind scheme and QUICK scheme in flow predictions. Convergence criteria were achieved after 1350 iterations.

5. *Computational Model Validation*

Model verification was carried out by predicting the single fluid flow in the computation domain. Fluids flowing in both the core and the annulus are the same. Fluid viscosity varies from μ = 1.0 cP (water) to μ = 18,000 cP (heavy oil). The results are compared with those of the well-known laminar and turbulent pipe flows. It is well established that velocity distribution in laminar pipe flow is a parabolic distribution.

Figure (3a) presents the predicted velocity profiles of the fully-developed laminar flow in oil pipes compared with well-known parabolic distribution. Three sets of flow data in D_o=3.04 cm pipe are presented for the flow of Fuel Oil (μ=1060 cP) at $Re = 51$, Heavy Oil-1 (μ=157 cP) at $Re = 356$, and Heavy Oil-3 (μ=3244 cP) at $Re = 75$. Comparison shows that predicted values are identical with the well-known parabolic distribution. This clearly demonstrates the ability of the developed model to predict the laminar flow accurately.

Figure (3b) presents the velocity profiles predictions in comparison with the typical velocity profile of turbulent flow. The results presented in wall layer coordinates ($U^+ vs. y^+$) shows excellent agreement in the viscous sublayer, buffer zone, and the log region area. It clearly demonstrates the accuracy of the model to predict turbulent flow especially in the near wall region. Predicted axial velocity profiles of turbulent pipe flow at $Re = 13100$, and 60800 shown in Figure (4) exhibit accurate values compared with the experimental data of Zagarola and Smits (1997) and Escudier and Presti [sited in Gibbings (1996)].

The friction coefficient of fully-developed pipe flow is computed for different values of Reynolds numbers from $Re = 4$ to 200,000. The results are shown in Figure (5). It is evident that the present numerical model gives accurate results for the turbulent flow as well as for the laminar flow. For laminar flow, the computed results of friction coefficient satisfy the well-known Hagen–Poiseuille relation;

$$C_f = 16/Re. \quad (12)$$

For turbulent flow, friction coefficient predictions are fairly represented by the Blasius' correlation:

$$C_f = 0.079/Re^{0.25} \quad (13)$$

Model predictions of velocity profiles and friction coefficient compared with the experimental data and the well-known flow relations showed that the present code using the standard k–ω model gives accurate results in fully-developed pipe flow.

6. *Results and Discussions*

Flow structure development of core-annular flow of heavy oil and water through 15.24 cm diameter pipe due to injecting water into the annulus region is investigated. Three sets of results with different core to outer diameter ratio α are presented. All have outer diameter D_o=15.24

cm, while the oil core diameters varies as D_c=12.7 cm, 14.0 cm and 14.7 cm, giving α=0.83, 0.92, and 0.96. Number of heavy oils of different viscosities ranging from μ=30 cP to μ=18000 cP are considered.

6.1. Oil Water Flow Structure

The development of axial and radial velocity profiles from section x=1.0 m at which water is injected, to the fully-developed one at some distance downstream is discussed. The development of turbulent kinetic energy, turbulence intensity, and strain rate are presented. Flow structure at oil-water interface is also investigated.

6.1.1. Oil-Water Flow Velocity Profiles

Figure (6) presents the development of velocity profiles of core-annular oil–water pipe flow with α=0.83. Both the average velocity of oil in the core U_o and water in the annulus U_w regions are U_o=U_w=2.0 m/s. Results at section x=0.75 m presents the velocity profile of the oil in the core before water injection, while the results at section x=1.0 m present the velocity profile of oil in the core and water in the annulus when water is injected. The results of other sections at x=1.05 m to the end of the test section x=10 m present the development of velocity profile of oil-water core-annular flow from the point of water injection.

Figure (6a) presents the velocity profiles development of core-annular pipe flow of mineral oil and water at Reynolds number Re=8738 based on Mineral oil's viscosity (μ=30 cP). Velocity distribution in the core region (ζ=0.0–0.833, ζ=r/R) at x=0.75 m and x=1.0 m are almost identical and a turbulent one, where the local Reynolds number Re_o=7281. The velocity distribution of water flow in the annulus region (ζ=0.833–1.0) at x=1.0 m is turbulent with peak to average velocity ratio ϕ=1.1 where local Reynolds number Re_w=12637. Velocity distribution in both the core and annular regions develops to form a fully-developed velocity profile at x=2.0 m. For the fully-developed profile, it is hardly to detect the core and annular region, and the velocity profile is a turbulent one. Identical fully-developed velocity profiles are found at any section x>2.0 m.

Figure (6b) presents the velocity profiles of oil-water flow at Re=3306. Oil considered has density ρ=911 kg/m^3 and viscosity μ=84 cP Similar to that of mineral oil shown in Figure (6a), the velocity distribution in the core region at sections x=0.75 m and x=1.0 m are almost identical and turbulent one, where the local Re_o=2755. The velocity distribution of water in the annulus region at x=1.0 m is turbulent one, and the fully-developed profile is a turbulent one with velocity ratio ϕ=1.2.

The development of velocity profiles of light crude oil-water pipe flow at Re=529 is presented in Figure (6c). Crude oil considered has viscosity μ=530 cP and density ρ=920 kg/m^3. In the core region at sections x=0.75 m and x=1.0 m, where the local Re_o=441, velocity profiles are laminar with peak to average velocity ratio ϕ=1.7. In the annulus region at x=1.0 m, where local Re_w=12637, water velocity profile exhibit turbulent distribution. The velocity distribution in both the core and annular

regions develops gradually to fully-developed profile at x>2.0 m. In the fully-developed profile, both the core and annular regions are distinguished, and the velocity distribution in the oil core is turbulent one with peak to average velocity ratio ϕ=1.2. Fully-developed velocity profiles are identical at any section x>5.0 m.

Velocity profiles of engine oil (μ=1060 cP and ρ=889 kg/m^3) and water at Re=256 is shown in Figure (6d). Velocity profiles development is similar to that of crude oil (μ=530). The velocity profiles in the core region at sections x=0.75 m and x=1.0 m show laminar velocity distribution, where local Re_o=213. Water velocity distribution in annulus at x=1.0 m is turbulent with ϕ=1.15. Figure (6d) shows that velocity profiles in core and annular regions develop to fully-developed one at x=5.0 m. In fully-developed profile, core and annular regions are distinguished, and the velocity distribution in the oil core is almost flat with little variations.

Figure (6e) presents the velocity profiles of heavy oil with viscosity μ=3244 cP and density ρ=954 kg/m^3 at Re=90. It shows that the development of velocity profiles of core-annular pipe flow of heavy oil-water is very similar to that of engine oil (μ=1060 cP) (shown in Figures (6d)), but with faster development towards the fully-developed profile. The fully-developed profiles occur at distance x<2.0 m. It is characterized by constant distribution in the core region and the oil core looks like a rigid body carried by the water flow in the annulus.

The development of velocity profiles of extra heavy oil (μ=18000 cP, ρ=960 kg/m^3) and water at Re=16 is shown in Figure (6f). Velocity profiles development is similar to that of the heavy oil (μ=3244 cP) shown in Figure (6e). Fully-developed velocity profiles occur at axial distance less than x=1.2 m.

Figure (7) presents the development of radial velocity profiles of oil–water core-annular flow through pipe of 15.24 cm outer and 14.0 cm core diameters, giving α=0.92. The average velocities of oil in the core and water in the annulus regions are equal U_0=U_w=3.0 m/s. Oils considered in this figure have viscosities, μ=30 cP, 1935 cP, 10230 cP, and 18000 cP. Figure (7a) shows the development of radial velocity profiles of oil-water, core-annular pipe flow of mineral oil (μ=30 cP) at Re=13106. At section x=1.0, the radial velocity profile of oil core shows flow outward peak near oil-water interface, while water at annulus shows another inward peak at oil-water interface. The profiles develop to uniform with zero value at sections x>2 m.

Figure (7b) shows the results crude oil of viscosity μ=1935 cP at Re=209. Radial velocity profiles show the same general trends exhibited in Figure (7a) for oils with lower viscosity. The only difference is that the peaks of radial velocity in both oil core and water annulus increases with oil viscosity.

The development of radial velocity profiles of extra heavy oil (μ=10230 cP) at Re=43 is presented in Figure (7c). It shows that the development of the radial velocity profiles of core-annular pipe flow of extra heavy oil-water is very similar to that of crude oil (μ=1935 cP). The peaks are much higher and moves away of the oil-water

interface. While, the radial velocity of water in the annulus region show almost identical distribution to those of crude oil7 (μ=1935 cP).

The radial velocity profiles of Fuel oil of viscosity μ=18000 cP and water at Re=24 is shown in Figure (7d). It shows that the development of the radial velocity profiles is very similar to that of heavy oil 7 (μ=10230 cP) shown in Figure (7c). The radial velocity of oil in the core shows higher values and the peaks are much higher and moves away of the oil-water interface.

6.1.2. Effect of Water Loading

The influence of water input ratio or the water loading ψ for the oil-water core annulus pipe flow upon the flow structure is investigated in the following section. The water loading ratio is defined as:

$$\psi = \frac{Q_w}{Q_w + Q_o} \qquad (14)$$

where, Q_w and Q_o are the volume flow rate of water and oils respectively.

Figure (8) presents the velocity profile development of oil-water core-annular flow in pipe $D_o = 15.24\,cm$ and $D_c = 14.0\,cm$ giving α=0.92. The heavy oil considered is engine oil (μ=1060 cP and density ρ=889 kg/m^3). The volume flow rate of oil in the core is kept constant at Q_o=110.9 m^3/hr. corresponding to an average velocity of U_o=2.0 m/s, while the volume flow rate of water in the annulus is varied such that the average velocity of water in the annulus varies as U_w= 0.5, 1.0, 1.5, 2.0, 2.5 and 3.0 m/s respectively.

Figure (8a) shows the development of velocity profiles of core-annular pipe flow at Re=226, at water loading ψ=0.04 that corresponds to U_w=0.5 m/s. In this case the velocity of water in the annulus is less than that of oil in the core. Velocity profiles in the core region at sections x=0.75 m and x=1.0 m, where local Re_o=235, exhibit laminar distribution. At x=1.0 m, water velocity profile in the annulus is laminar, where local Re_w=1542. The low velocity water in the annulus is drawn by the high velocity oil in the core that causes water in annulus to be accelerated to match oil velocity in the core. Velocity profiles in both core and annular regions at sections 1.0 m< x <3.0 m, develop gradually to form fully-developed velocity profile at x=3.0m. For the fully-developed profile at $x > 3m$, both the core and annular regions are distinguishable, and the oil velocity in the core region is almost constant with little variations, while the velocity distribution in the annulus is a turbulent one with sharp increase near the wall to maximum at oil water interface.

Figure (8b) shows the velocity profile development at water loading ψ=0.08 that corresponds to water velocity in the annulus U_w=1.0 m/s. Similar to Figure (8a), the velocity profiles in the core region at sections x=0.75 m and x=1.0 m, exhibit laminar distribution, while water velocity profile in annulus at x=1.0 m, is turbulent, where local Re_w=3085. For the fully-developed profiles at x>3.0 m, both ore and annular regions are distinguishable, and oil velocity distribution in the core is almost constant with little variations, while the velocity distribution in the annulus is a

turbulent one with sharp increase near the wall to maximum at oil water interface.

Figure (8c) shows the velocity profiles at water loading ψ=0.12, Re_w=4627, still water velocity in the annulus is less than that of oil in the core. The low velocity water in annulus is drawn by the high velocity oil flow in the core that causes the velocity of water in annulus to be increased to match oil velocity in the core. This is clearly demonstrated by stretching the velocity of water at the oil-water interface until it reaches the fully-developed value at x=3.0 m. Fully-developed profile in the core region is almost constant with little variations, while the velocity distribution in the annulus is turbulent.

Figure (8d) shows the velocity profiles of oil-water core-annular pipe flow at water loading ψ=0.16, where the velocity of water in annulus is equals to that of oil in the core. Results are very similar to that given in Figure (8c).

Figure (8e) shows the velocity profiles at water loading ψ=0.19 that corresponds to U_w=2.5 m/s. The velocity of water in the annulus is higher than that of oil in the core. The high velocity water in annulus is slowed down by the low velocity oil in the core that causes the velocity of water in annulus to be suppressed to match oil velocity in the core. Similar results are exhibited in Figure (8f) at water loading ψ=0.22 which corresponds to U_w=3.0 m/s.

6.1.3. Turbulent Kinetic Energy Profiles

Figure (9) presents the turbulent kinetic energy k profiles of oil–water core-annular flow through a pipe of α=0.92. The average velocity of oil in core and water in annulus regions are U_o=U_w=3.0 m/s. Oils with different viscosities are studied.

Figure (9a) shows the turbulent energy k profiles of core-annular pipe flow of mineral oil (μ=30 cP) at Re=13106. The results show that k profiles in the core region at sections x=0.75 m and x=1.0 m, where the local Re_o=10922, exhibit turbulent distribution with peak value near the wall. In the annulus region, at x=1.0 m, k profile of water, where local Re_w=18955 is turbulent with two peaks near wall and at oil-water interface. Turbulent energy profiles in both the core and annular regions develops gradually to form single profile at sections up to x=2.0 m. At sections x>2 m, k exhibits only one peak near solid wall of outer pipe, and it is hardly to detect the core and annular region.

Figure (9b) presents the developments of k profiles of core-annular pipe flow of heavy oil (μ=256 cP) at Re=1524. In the core region at sections x=0.75 m and x=1.0 m, where local Re_o=1400, turbulent kinetic energy k profiles are almost identical and exhibits zero values. However, in annulus region at x=1.0 m, where local Re_w=9254, k profile of water exhibits two peaks.

Figure (9c) presents the results of crude oil (μ=1935 cP) at Re=192. For such higher viscosity oil, the profile is very similar to that presented in Figure (9b). The only difference is that, at sections x >2.0 m, turbulent energy k in the core region is lower with a value of k≈0.005 m^2/s^2. Turbulent kinetic energy profiles of extra heavy oil (μ=18000 cP) and water flow at Re=24 is given in Figure (9d). Results show that the distribution of turbulent energy k of

extra heavy oils is similar to those of lower viscosity oils presented in Figures (9b), and (9c). Turbulent energy exhibits lower values for the oil core flow as the viscosity increased, while k exhibits same values for the water flow in the annulus. It has been demonstrated that the peak of k at oil-water interface is reduced by increased oil viscosity.

6.1.4 Strain Rate Profiles

Figure (10) presents the strain rate γ profiles of oil–water core-annular flow through a pipe of α=0.92. The average velocity of oil core and water annulus flows are 3.0 m/s. Strain rate γ profiles considered at sections x=1.0 m to x=10 m. The results of heavy oils of viscosity μ=256 cP, and μ=10230 cP, are considered.

Strain rate γ profile of low viscosity oils (μ=256 cP) is shown in Figure (10a). At section x=1.0 m, the results show that γ profiles exhibit two peak values, one near the wall of the pipe, and the other at oil-water interface. It also shows that strain rate profiles in both the core and annular regions develop to fully-developed profile at x>1.5m. In the fully-developed γ profile, still two peaks are found, a high one in the near wall region, and a smaller one at oil-water interface. The peak at oil water interface decreases as the flow moves away downstream and the γ profile develops to fully-developed one.

Figure (10b) shows the strain rate γ profiles of extra heavy oil (μ=10230 cP) Results show that γ profiles are very similar to those of low viscosity oil (μ=256 cP) presented in Figure (10a). It shows that the distribution of strain rate γ in water annulus is identical and is independent of oil viscosity. However, the strain rate γ distribution in oil core depends on oil viscosity. Increasing oil viscosity suppresses the strain rate in oil core.

6.2. Flow Structure at Oil -Water Interface

It has been demonstrated that major changes in flow structure occur at the oil-water interface. Therefore, it is essential to investigate the flow structure in this region. Figure (11a) presents the axial development of the velocity at the interface of oil and water for α=0.83. Heavy oils of different viscosities are considered. The results show that at oil-water interface, the velocity develops to constant value as they move away from the point of first contact. They show also that as oil's viscosity increases, the development becomes faster.

Figure (11b) presents the strain rate γ axial development at the interface of oil and water for α=0.83. Oils of different viscosities; μ=30 cP to 18000 cP are considered. The results show that at oil water interface, the strain rate γ develops to constant value as it moves away of the point of first contact at x=1 m. They show that γ starts with very high value at x=1 m, then decreases to a minimum value somewhere downstream and increases again to asymptotic values. It is interesting to note that the constant value of γ is the same for all heavy oils considered except for mineral oil of μ=30 cP. It may be due to the fact that the flow in the oil core is laminar, while it is turbulent in mineral oil-water flow.

Figure (12) presents the axial development of the turbulent kinetic energy

k and the turbulent intensity λ, at the surface of oil-water interface. Heavy oils of different viscosities μ=30-18000 cP are considered. The results show that there is a general trend in the development of both the turbulent kinetic energy k, and turbulence intensity λ at oil-water interface. Both k and λ develop to constant values as they moves away downstream the point of first contact of oil and water at x=1 m. Both k and λ starts with very high value at x=1, then decrease to minimum somewhere downstream and increase again to asymptote constant values. Such constant or asymptotic values of k and λ depend on the viscosity of the heavy oil considered. They decrease with the increase of viscosity.

The influence of water loading ψ on turbulent energy k at the oil–water interface of in pipe with α=0.92 is shown in Figure (13). Oils investigated are crude oil (μ=530 cP) and engine oil (μ=1060 cP). The volume flow rate of oil in pipe core is kept constant at an average velocity of U_o=2.0 m/s, while the volume flow rate of water in the annulus is varied giving average velocity as U_w=0.5-3.0 m/s, corresponding to water loading ψ=0.04-0.22 respectively.

Figure (13a) shows the development of turbulent energy at oil-water interface. It shows that for any value of water loading ψ, the turbulent kinetic energy k develops to constant value through a peak very close to x=1.0 (point of water injection), followed by a minimum. Increasing water loading ψ by increasing the incoming water velocity, the minimum values of k move away downstream, and the development of k becomes slower. The developed value of k is independent of water loading ψ. Similar results are shown in Figure (13b) when the turbulent kinetic energy at oil-water interface is plotted as function of axial distance for the flow of engine oil and water.

7. Conclusions

Based on the above discussion for the core-annular flow of heavy oils and water flow in pips, the followings are concluded

1. Depending on the viscosity of the oil, the velocity profiles in both the core and annular regions at sections x>1 develops to a fully-developed one at some distance downstream the section at which water is injected (x=1).
2. Fully-developed profiles of oil-water core-annular flow show distinguishable core and annular regions, and the oil velocity distribution in the core region is almost constant with little variations, while the velocity distribution in the annulus looks like a turbulent one with sharp increase near the wall to maximum at oil water interface.
3. Increasing oil's viscosity μ>3000 cP, velocity profiles develops faster. Fully-developed profiles exhibit almost constant velocity distribution in the oil core and the core looks like a rigid body carried by the annular water flow.
4. Water loading ψ greatly affects the development of flow structure in the annulus and at oil-water interface. The fully-developed velocity profiles are not affected by ψ.
5. When injecting water into the annulus at velocities lower than that of oil, water in the annulus is drawn by the oil

flow in the core, to match oil velocity. However when water injected at velocities higher than that of oil, the high velocity water in annulus is slowed down by the low velocity oil flow in the core to match oil velocity in the core.

6. Turbulent kinetic energy k profiles exhibit very sharp peak in core region at oil-water interface, and another distinct peak near wall in the annulus region. Profiles develop gradually to form single profile that it is hardly to detect the core and annular region, and k exhibits only one peak near wall.

7. Strain rate γ profiles of oil–water core-annular flow exhibit two peaks, one near the wall of the pipe and the other at oil-water interface. Strain rate γ in water annulus is independent of oil viscosity, while in oil core, it depends on oil viscosity. Increasing oil's viscosity suppresses the strain rate in oil core.

8. At oil-water interface, the axial velocity, the strain rate γ, the turbulent kinetic energy k, and turbulent intensity λ develop to a constant value as it moves away of the injection point. The strain rate γ, turbulent energy k, and turbulent intensity λ, start with high values then decrease to minimum somewhere and increase again to asymptotic values.

Nomenclature

C_f Friction coefficient
D_c Oil core diameter
D_o Outer pipe diameter
G_k Generation of the turbulence kinetic energy k
G_ω Generation of specific dissipation rate of turbulence ω
k Turbulent kinetic energy k
m The mass flow rate m in kg/sec,
Q_o the volume flow rate of oils
Q_w the volume flow rate of water
r Radial coordinate
R Pipe radius
R_o Outer pipe radius
Re Reynolds number of the flow, $\mathrm{Re} = \rho.U.d_h / \mu$
Re_o Reynolds number of oil flow, $Re_o = \rho_o.U_o.d_h/\mu_o$
Re_w Reynolds number of oil flow, $Re_w = \rho_w.U_w.d_h/\mu_w$
S_k User-defined source term of k.
S_ω User-defined source term of (ω).
u Axial velocity, (m/s)
u_i The ith component of the velocity, i.e. along the r, θ, z direction.
$\overline{u_i}$ The time - mean averaged velocity components in the ith direction.
u_i' The fluctuating velocity components in the ith direction.
$\overline{\rho u_i' u_j'}$ Reynolds stresses, turbulent normal and shear stress terms.
$\vec{U}$ Velocity vector of the flow,
U_o Axial velocity of oil in the core at inlet
U_o Axial velocity of water in the annulus at inlet
U Average axial flow velocity
U^+ Wall parameters dimensionless velocity $U^+ = U/u^*$
u^* Shear velocity given by $u^* = \sqrt{\tau_w/\rho}$
x Coordinate in x direction,
y Normal distance from wall
y^+ wall parameters dimensionless normal distance from wall
Y_k Dissipation of turbulent kinetic energy k
Y_ω Dissipation of the specific dissipation rate (ω)

$\rho u_i' u_j'$	Reynolds stresses, turbulent normal and shear stress terms.
α	Core to outer diameters ratio $\alpha=D_c/D_o$
ε	Turbulent specific dissipation rate (ε)
γ	Strain rate (1/s).
λ	Turbulent intensity λ,
μ	Viscosity of the fluid ((N/m^2.s)
μ_t	Turbulent (eddy) viscosity,
ρ	Fluid density (kg/m^3)
ϕ	Average velocity ratio, $\phi=(Uc/Uav)$
ψ	Water input ratio or water loading ratio,
τ	Shear stress, (N/m^2)
τ_w	Wall shear stress
ω	Specific dissipation rate of turbulence.
ξ	Radial Distance $\zeta=r/R$

References

Bai, R., Chen K., and Joseph, D.D., Lubricated pipelining: stability of core-annular flow: Part 5, Experiments and comparison with theory, J. Fluid Mechanics, 240, (1992), pp. 97–132

Bannwart, A.C., Modeling aspects of oil–water core–annular flows, J. Petroleum Sci. Eng. 32 (2001), pp. 127–143

Bensakhria A., Peysson Y., and Antonini G., Experimental study of pipeline lubrication of heavy oil transport, Oil Gas Science Technology Rev. IFP 2004; 59 (5), 523–33.

Brauner N., and Ullmann, A., Modeling of phase inversion phenomenon in the two-phase flows, Int. J. Multiphase Flow, 28 (6) (2002), pp. 1177–1204.

Charles, M.E., Govier G.W. and Hodgson, G.W., The horizontal pipeline flow of equal density of oil–water mixtures, Cand. J. Chem. Eng., 39 (1961), pp. 17–36.

Clark A.F., and Shapiro A., Method of pumping viscous petroleum, U.S. Patent no. 2,533, 878 (1949).

Fluent, User's Guide FLUENT 6.3.26. Fluent Inc., Canonsburg, PA, (2006).

Ghosh, S., Mandal, T.K., Das, G., and Das, P.K., Review of oil water core-annular flow, J. Renewable Sustainable Energy Rev., 13, (2009), pp. 1957-1965.

Gibbings, J. C., On the measurement of skin friction from the turbulent velocity profile, Flow Meas. Instrum., Vol. 7, No. 2, (1996), pp. 99-107.

Grassi, B., Strazza D., and Poesio, P., Experimental validation of theoretical models in two-phase high-viscosity ratio liquid–liquid flows in horizontal and slightly inclined pipes, Int. J. Multiphase Flow 34 (10) (2008), pp. 950–965.

Huang A., Christodoulou C., and Joseph, D.D., Friction factor and hold up studies for lubricated pipelining part. 2: Laminar and k-ε models of eccentric core flow, Int. J. Multiphase Flow, 20 (3), (1994), pp. 481–491.

Joseph, D.D., Bai, R., Chen, K.P., and Renardy, Y.Y., Core annular flows. Annual Review of Fluid Mechanics 29, (1997), pp.65–90

Ko T., Choi H.G., Bai R. and Joseph D.D., Finite element method simulation of turbulent wavy core–annular flows using a k–ω turbulence model method, Int. Journal of Multiphase Flow, 28, (7), (2002), pp. 1205-1222.

Menter, F.R., Two equation eddy viscosity turbulence models for engineering applications, AIAA J. 32 (8), (1994), pp. 1598–1605

Miesen R., Beijnon G., Duijvestijn P.E.M., Oliemans R.V.A., and Verheggen T., Interfacial waves in core-annular flow, J. Fluid Mechanics, 238, (1993), pp. 97–117.

Oliemans, R.V.A., Ooms, G., Wu, H.L., and Duijvestijn, A., Core - annular oil / water flow: turbulent lubricating film model and measurements in a 5 cm pipe loop, Int. J. Multiphase Flow 13 (1987), pp. 23–31.

Oliemans, R.V.A., The lubricating-film model for core-annular flow. Ph.D. Thesis, (1986), Delft University of Technology, The Netherlands.

Ooms, G., Seoal, A., Vanderwees, A.J., Meerhoff R., and Oliemans R.V.A., A theoretical model for core-annular flow of a very viscous oil core and a water annulus through a horizontal pipe, Int. J. Multiphase Flow, 10 (1984) 41– 60.

Ooms, G., and Poesio, P., Stationary core-annular flow through a horizontal pipe, Physical Review E 68, 066301, (2003)

Ooms, G., Vuik, C., and Poesio, P., Core-annular flow through horizontal pipe-hydrodynamic counter balancing of buoyancy force on core, Physics of Fluids 19, 092103, (2007).

Rodriguez O.M.H., Bannwart A.C. and Carvalho C.H.M., Pressure loss in core-annular flow: Modeling, experimental investigation and full-scale experiments, J. Petroleum Science and Engineering, Volume 65, Issues 1-2, (2009), pp. 67-75

Rovinsky, J., Brauner, N., and Moalem, M.D., Analytical solution for laminar two-phase flow in a fully eccentric core-annular configuration, Int. J. Multiphase Flow 23(3), (1997), 523-543.

Sotgia, G., Tartarini, P., and Stalio, E., Experimental analysis of flow regimes and pressure drop reduction in oil–water mixtures, Int. Journal of Multiphase Flow 34 (2008), pp 1161–1174

Strazza, D., Grassi, B., Demori, M., Ferrari, V., and Poesio, P., Core-annular flow in horizontal and slightly inclined pipes: Existence, pressure drops, and hold-up, Chemical Engineering Science, 66, (2011) pp 2853–2863

Torres-Monzon, C.F., Modeling of oil-water flow in horizontal and near horizontal pipes, PhD Mechanical Engineering, University of Tulsa, (2006).

Xu, X.X., Study on oil–water two-phase flow in horizontal pipelines, Journal of Petroleum Science and Engineering, Volume 59, Issues 1-2, (2007), pp 43-58

Wilcox. D. C., "Turbulence Modeling for CFD", *DCW Industries Inc.*, La Canada, California, (1998).

Zagarola, M.V., and Smits, A. J., J. Fluid Mech. 373, 33 (1997)

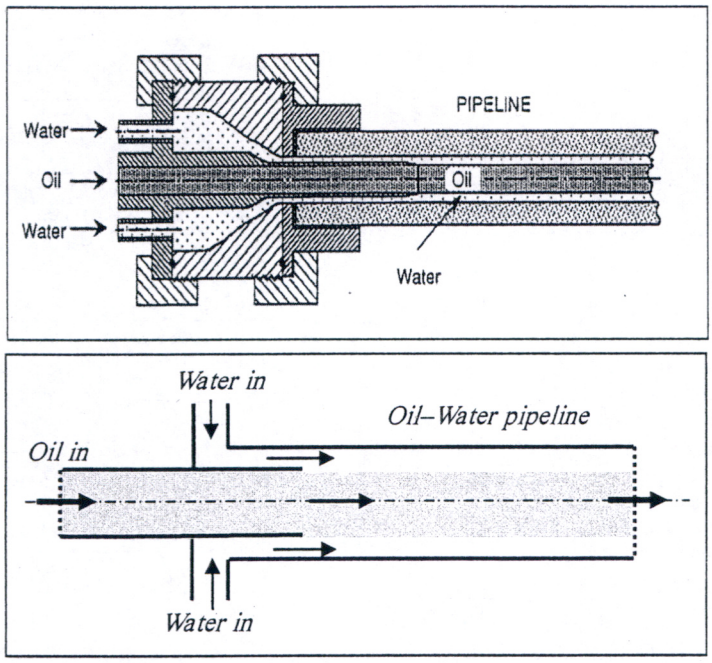

Figure (1)
Schematic description of the core-annular pipe flow

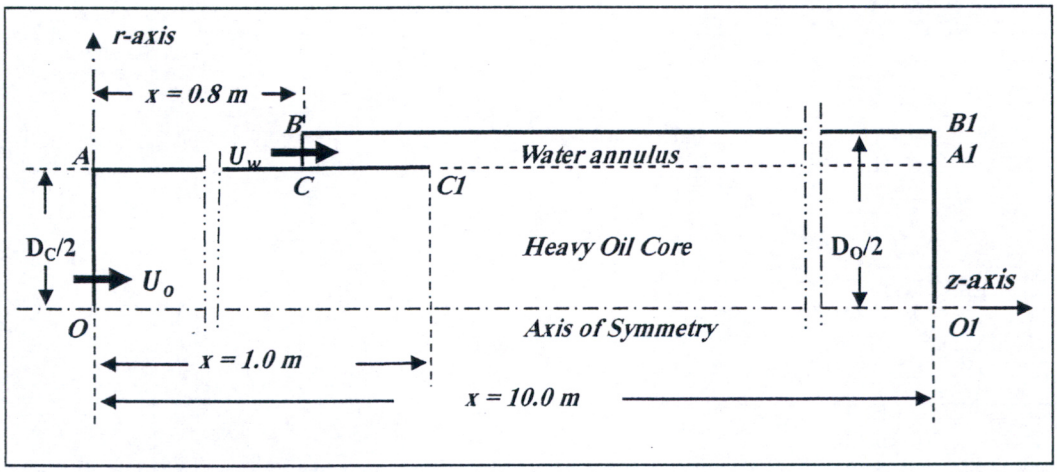

Figure (2)
Flow geometry, coordinate system, and computational domain

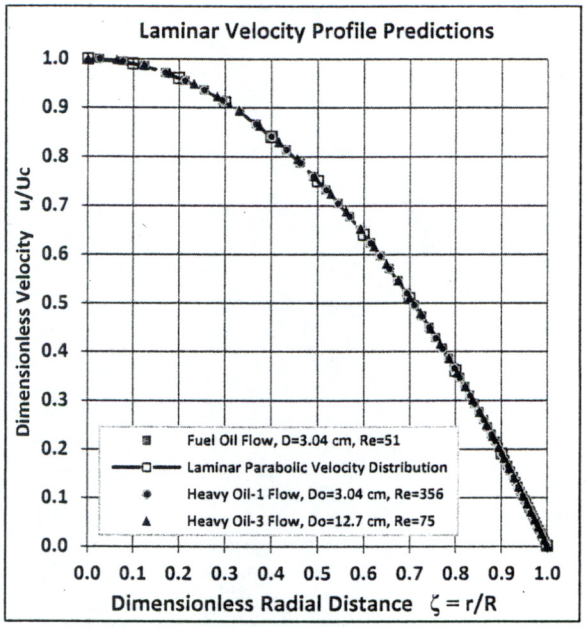

Figure (3a) Laminar Flow

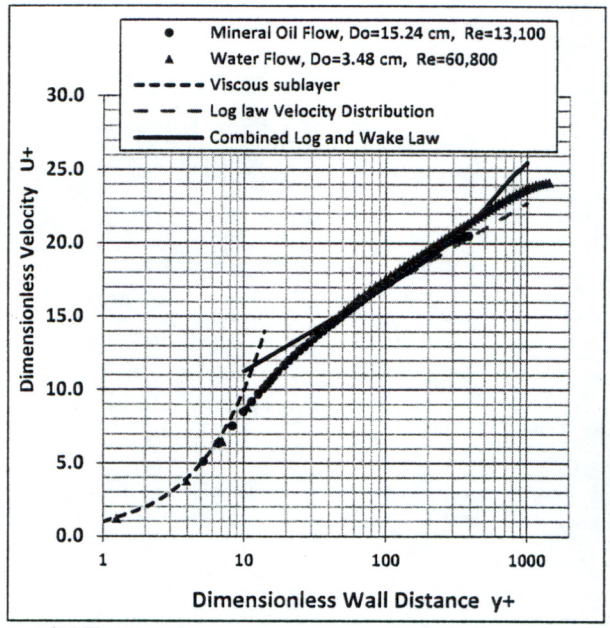

Figure (3b) Turbulent Flow

Figure (3)
Velocity profiles predictions for laminar and turbulent pipe flows in comparison with typical velocity distributions

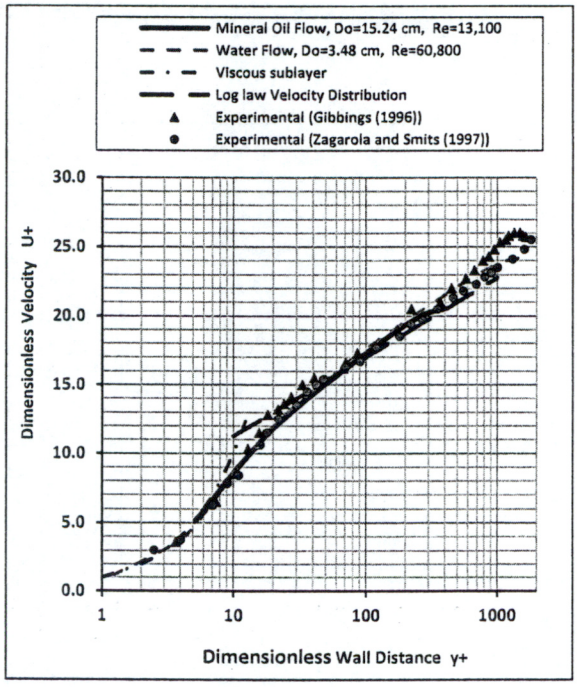

Figure (4)
Velocity distribution U^+ as function of wall distance y^+ compared with the experimental data of Zagarola and Smits (1997), Escudier and Presti [sited in Gibbings (1996)]

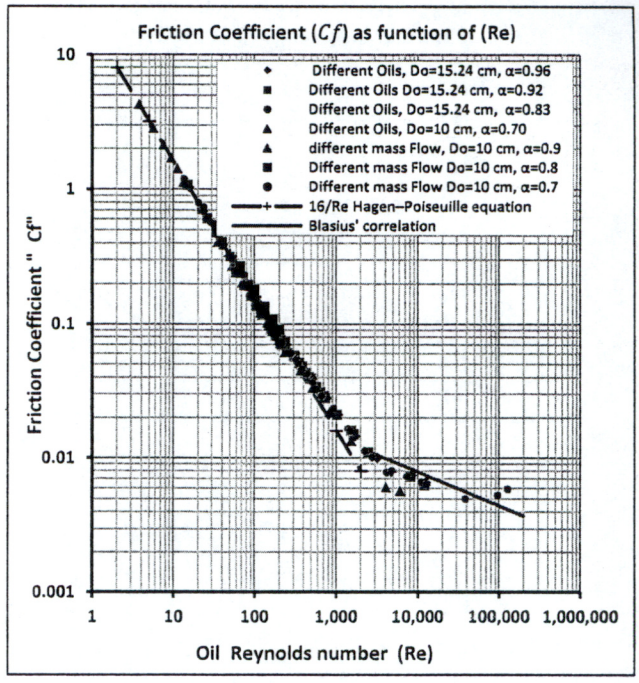

Figure (5)
Friction Coefficient (C_f) vs. Reynolds number (Re) in the fully-developed pipe flow,
– – – Hagen–Poiseuille for laminar flow;
—— Blasius correlation for turbulent flow

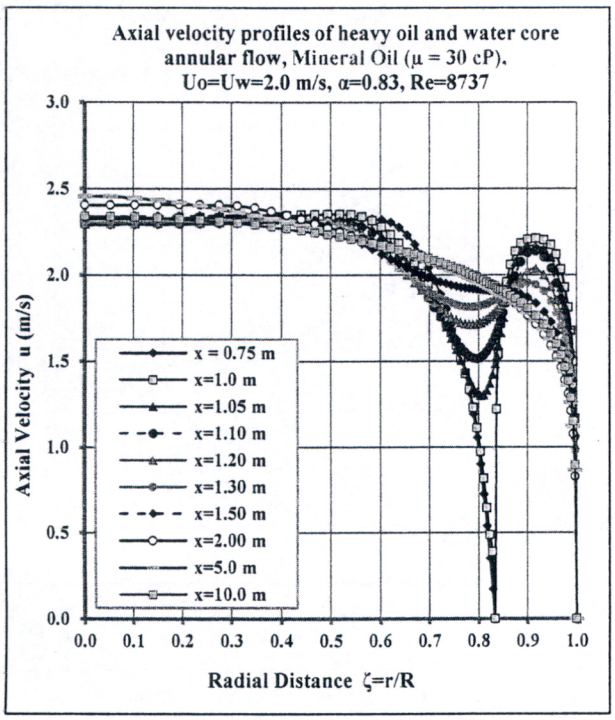

Figure (6a) Mineral Oil (μ=30 cP)

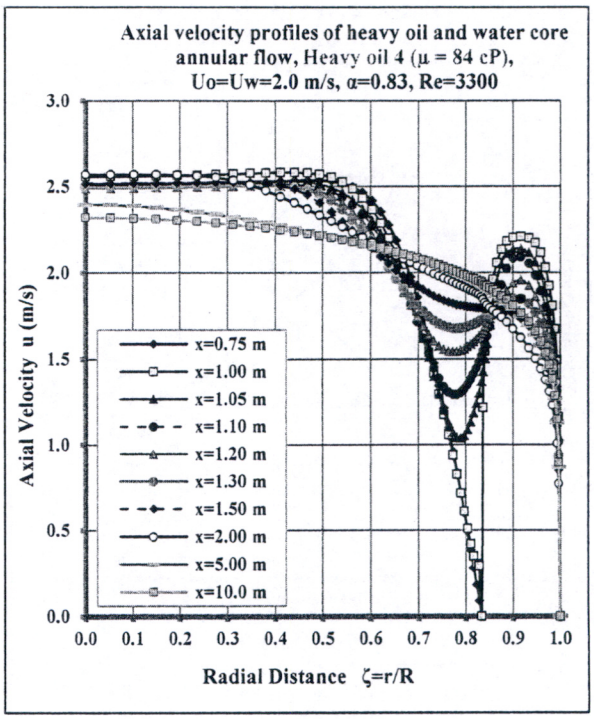

Figure (6b) Heavy oil 4 (μ=84 cP)

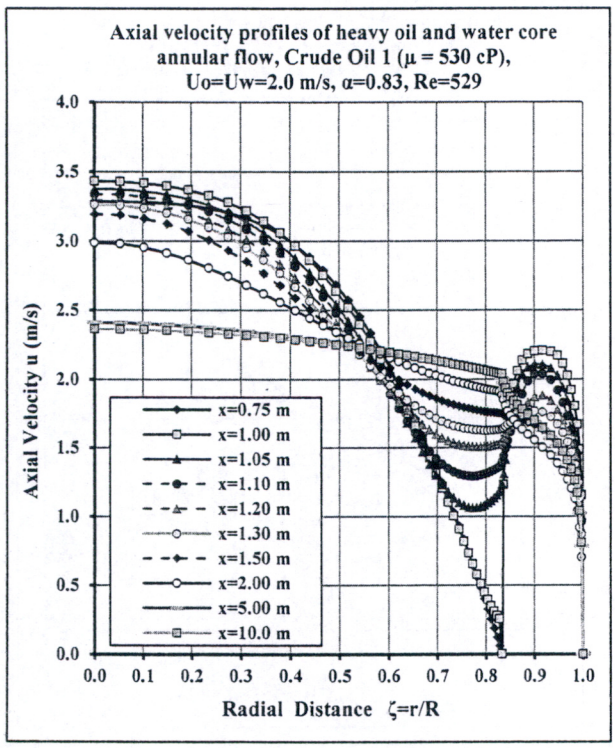

Figure (6c) Crude oil (μ=530 cP)

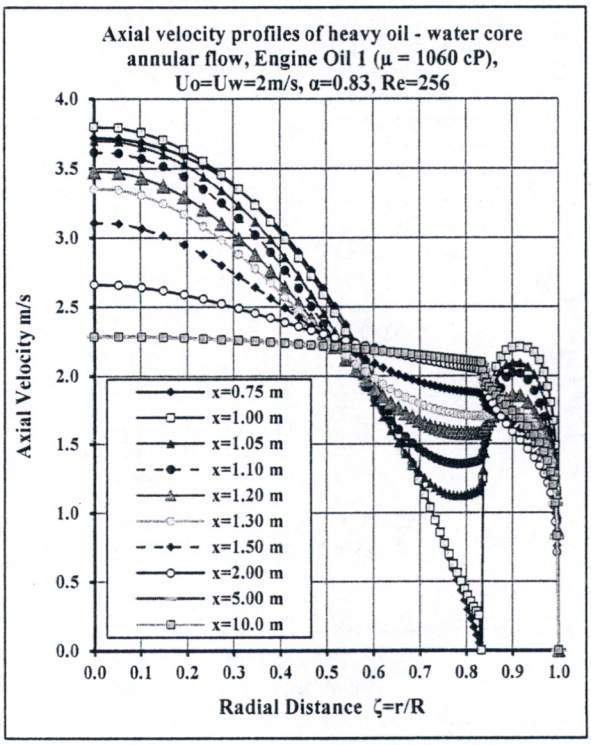

Figure (6d) Engine oil (μ=1060 cP)

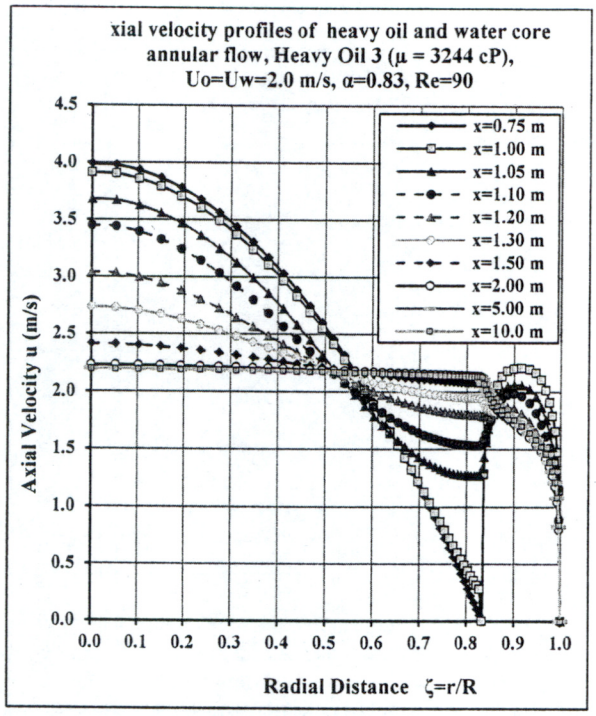

Figure (6e) Heavy oil (μ=3244 cP)

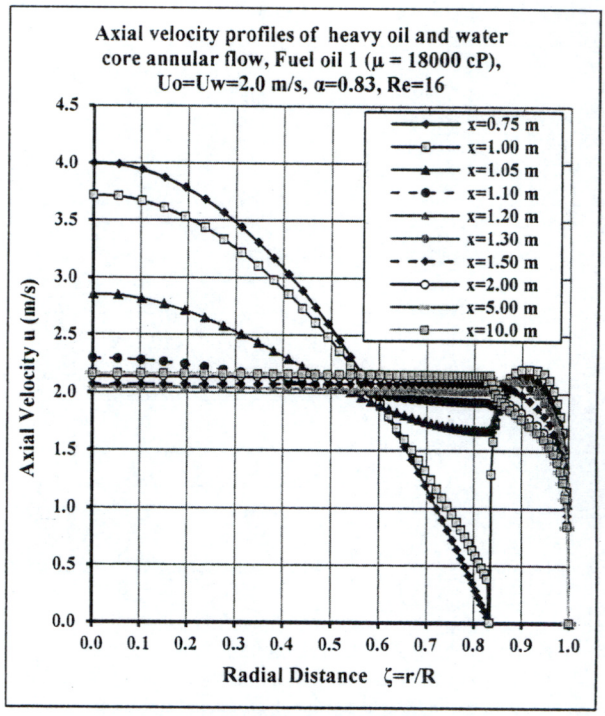

Figure (6f) Extra heavy oil (μ=18000 cP)

Figure (6)
Axial velocity profiles development of core-annular pipe flow of oil-water system, α=0.83

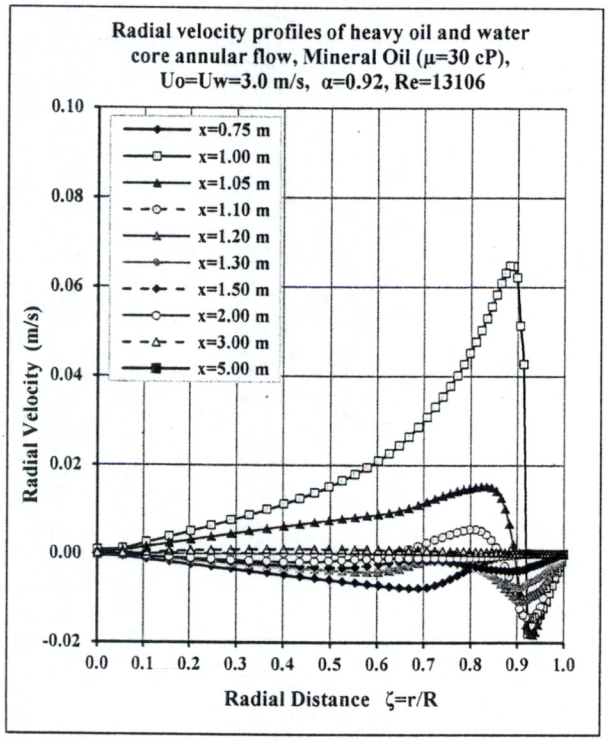

Figure (7a) Mineral oil (μ=30 cP)

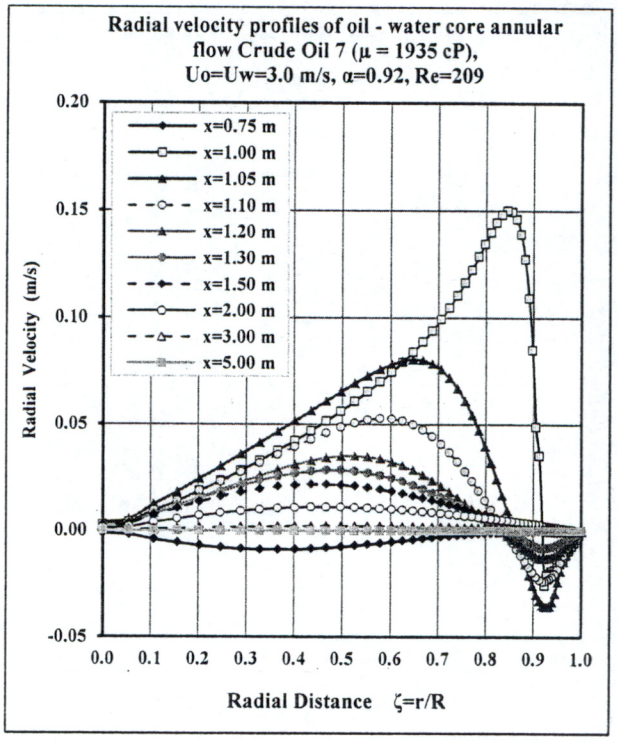

Figure (7b) Crude oil 7 (μ=1935 cP)

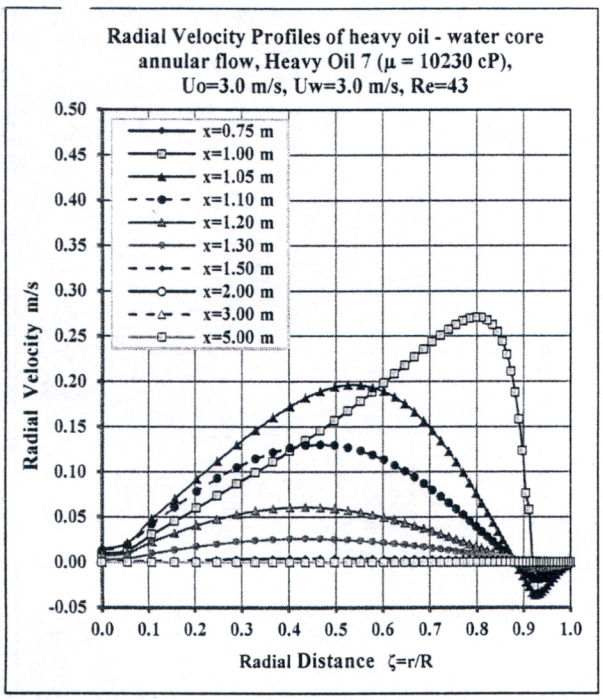

Figure (7c) Heavy Oil-7 (μ = 10230 cP)

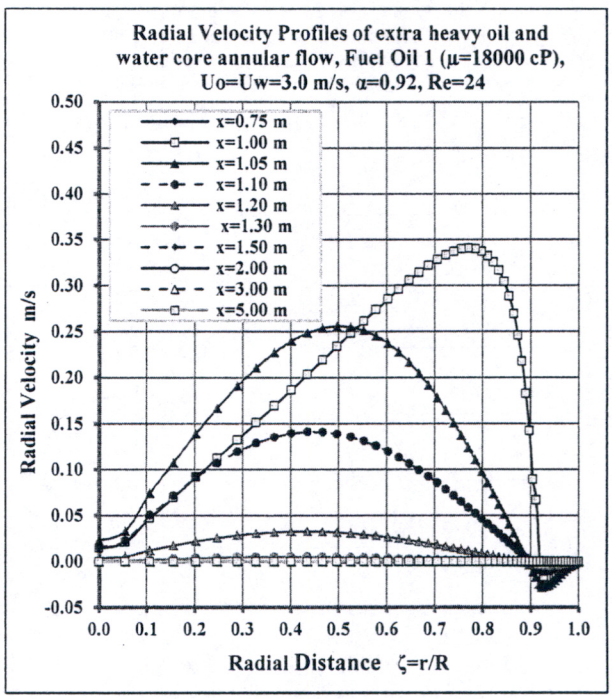

Figure (7d) Fuel Oil-1 (μ=18000 cP)

Figure (7)

Radial velocity profiles of oil-water core-annular pipe flow, α=0.92

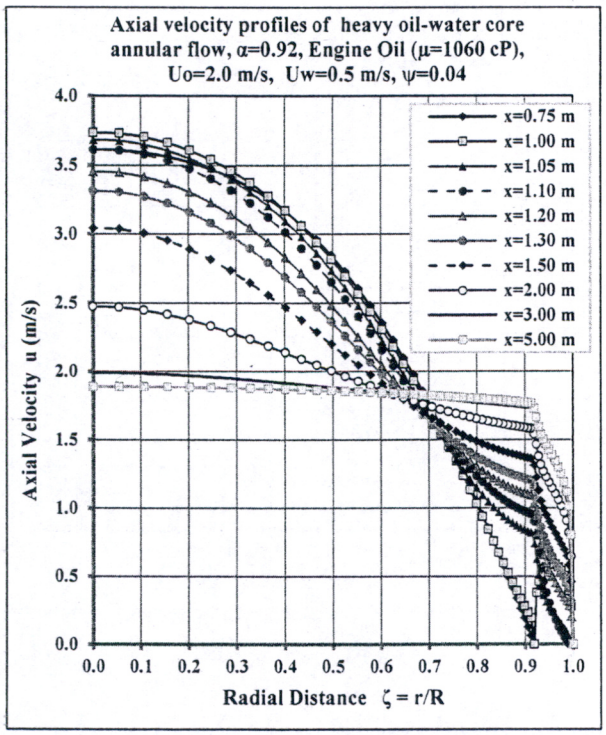

Figure (8a) ψ=0.04

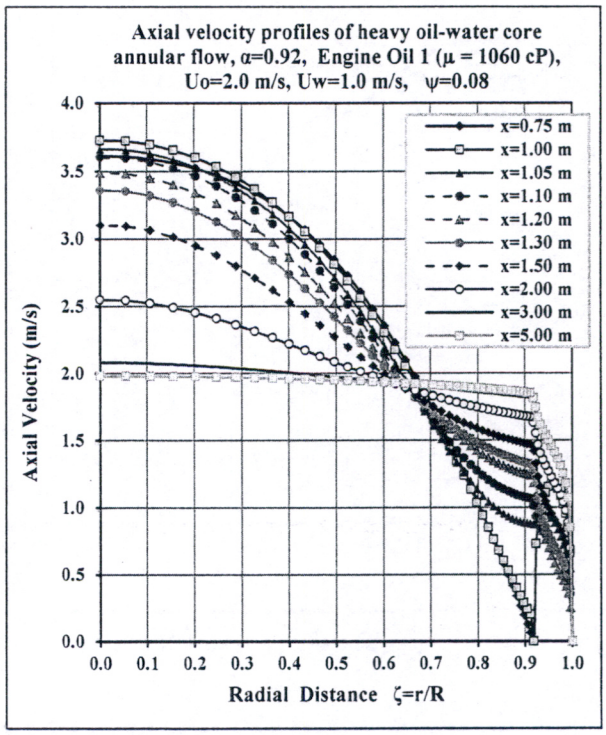

Figure (8b) ψ=0.08

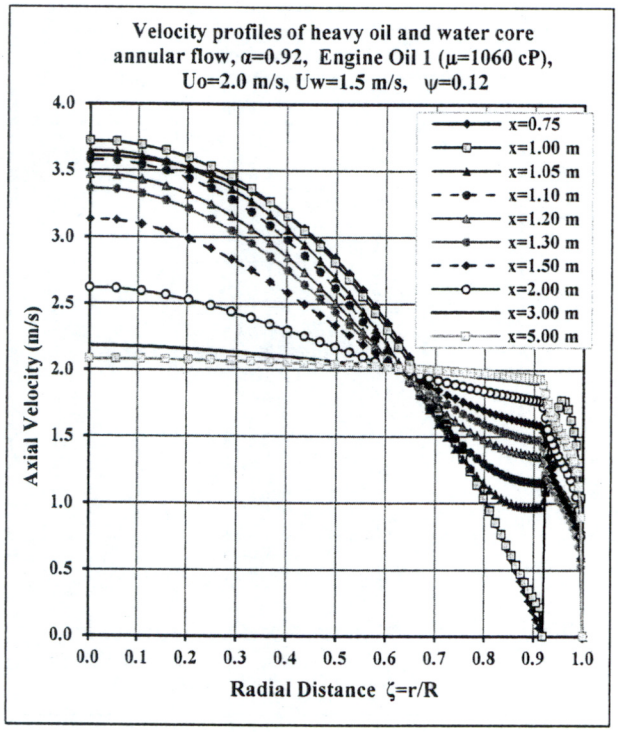

Figure (8c) ψ=0.12

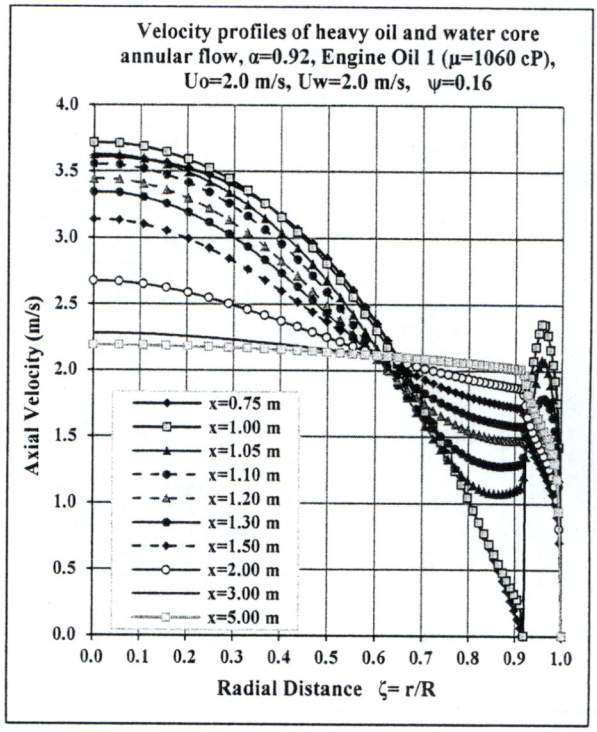

Figure (8d) ψ=0.16

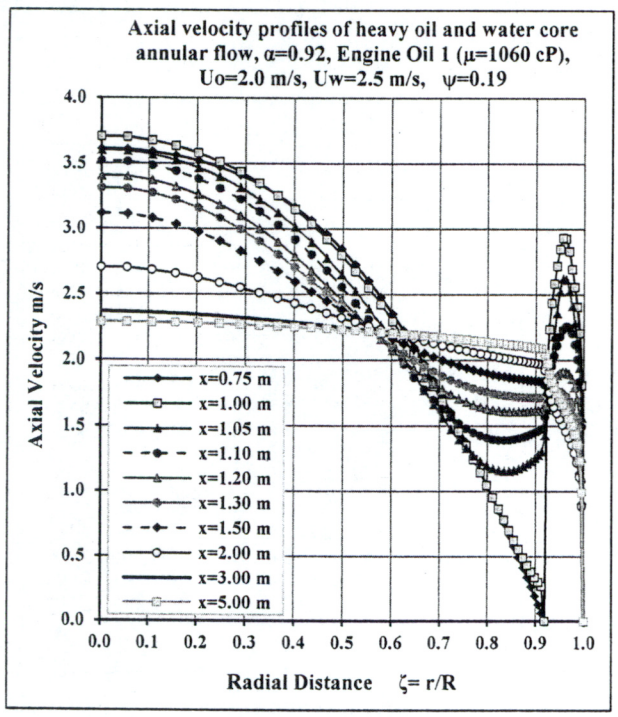

Figure (8e) ψ=0.19

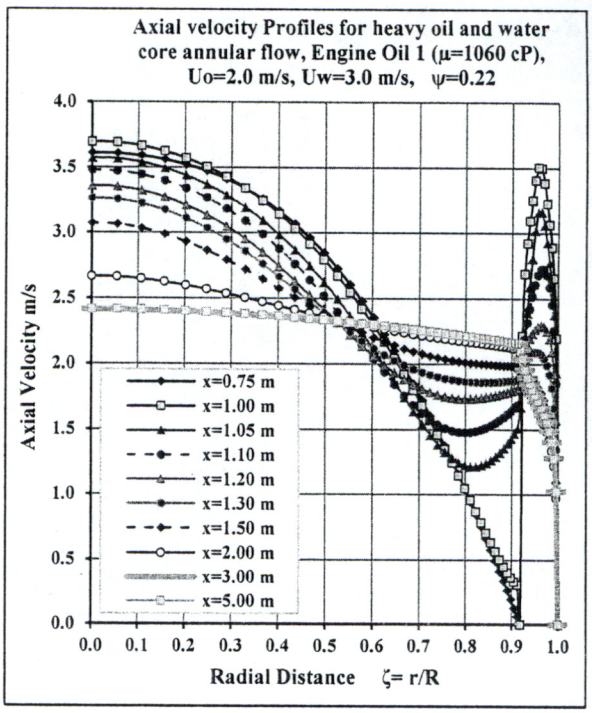

Figure (8f) ψ=0.22

Figure (8)

Axial velocity profiles of core-annular pipe flow of heavy oil and water, α=0.92, different ψ

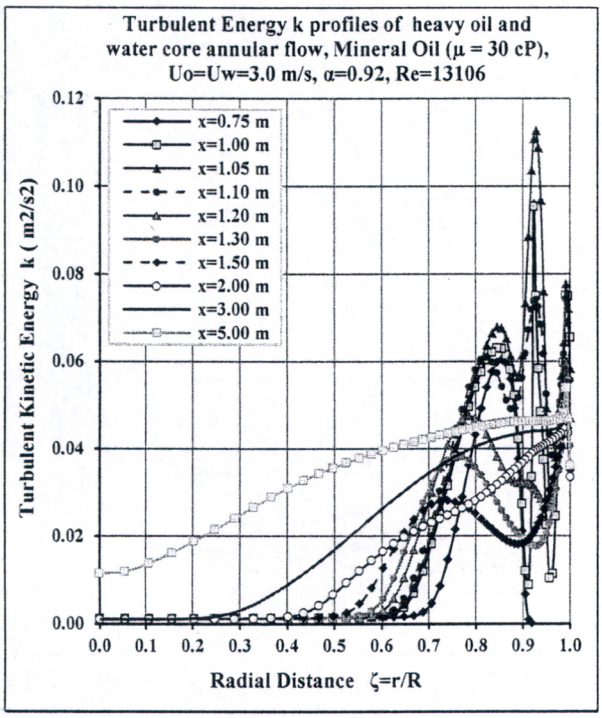

Figure (9a) Mineral Oil (μ=30 cP)

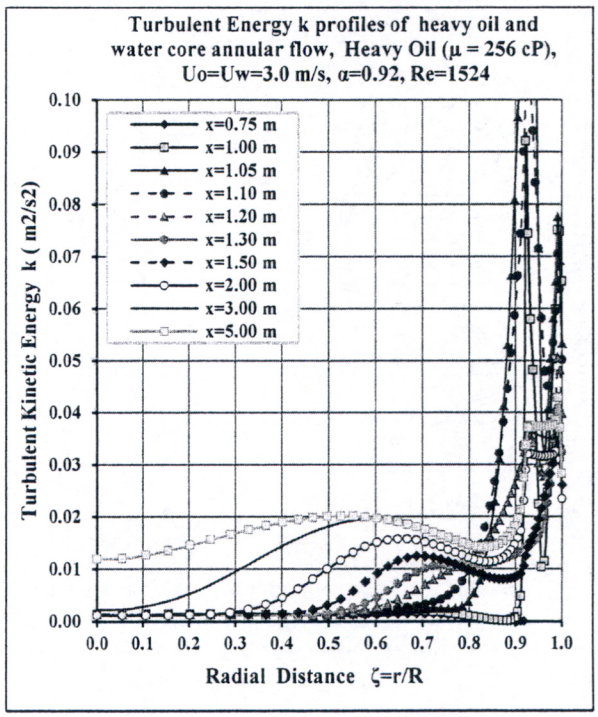

Figure (9b) Heavy Oil 5 (μ = 256 cP)

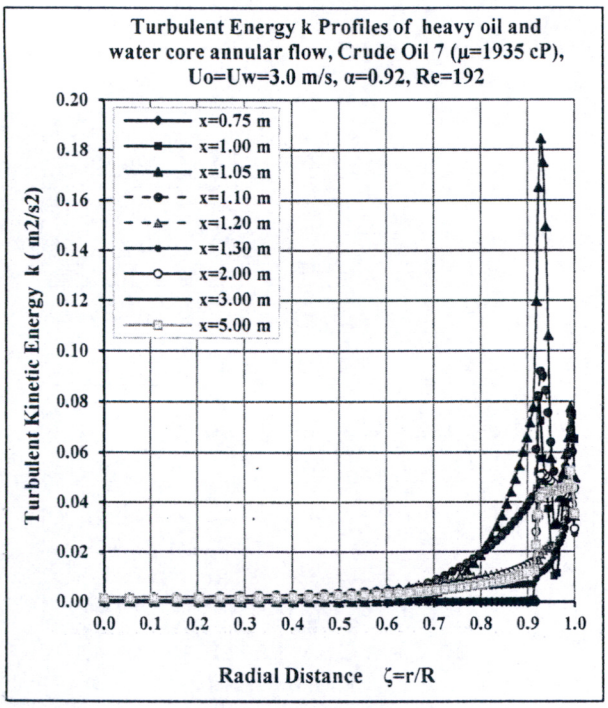

Figure (9c) Crude Oil 7 (μ=1935 cP)

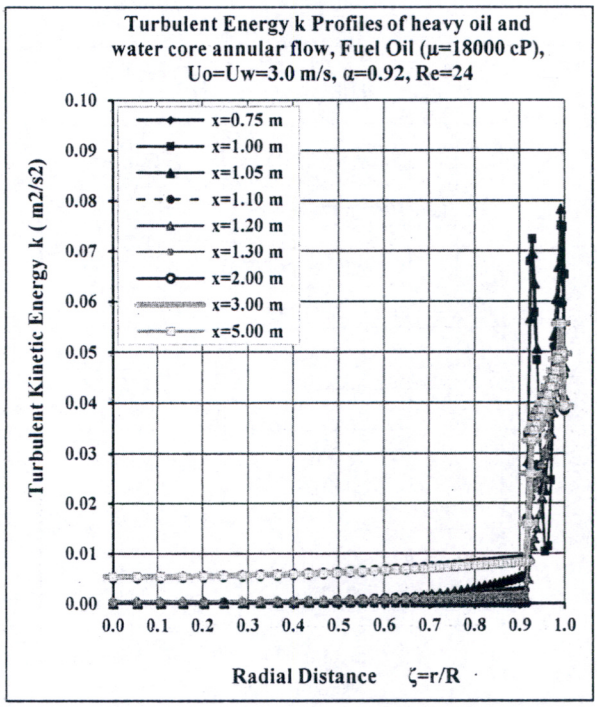

Figure (9d) Fuel Oil (μ=18000 cP)

Figure (9)

Turbulent Kinetic Energy k profiles of core-annular pipe flow of oil and water, α=0.92

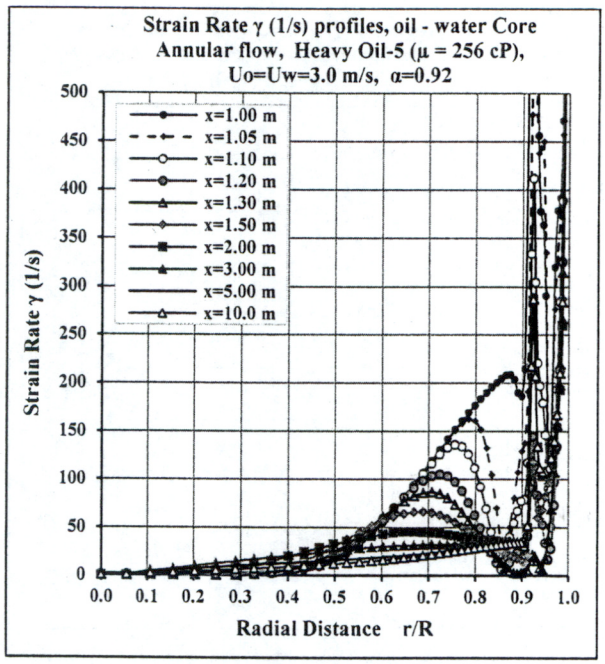

Figure (10a) Heavy oil-5 (μ=256 cP)

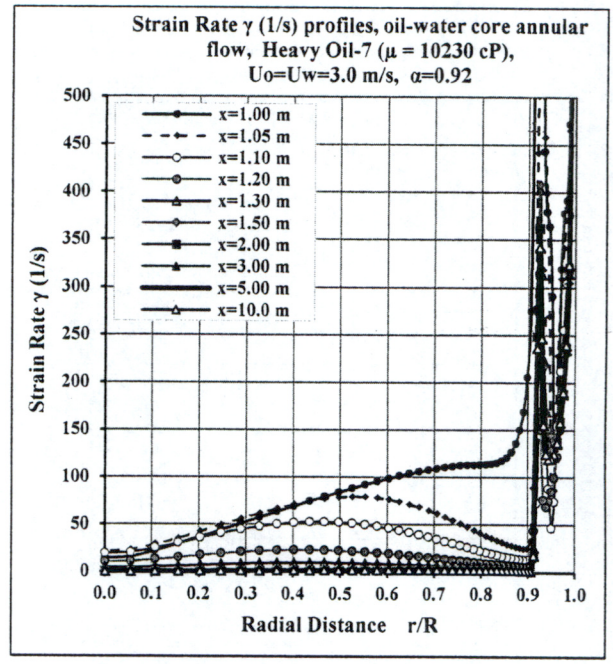

Figure (10b) Heavy oil-7 (μ=10230 cP)

Figure (10)
Strain rate γ profiles of oil-water core-annular pipe flow, α=0.92

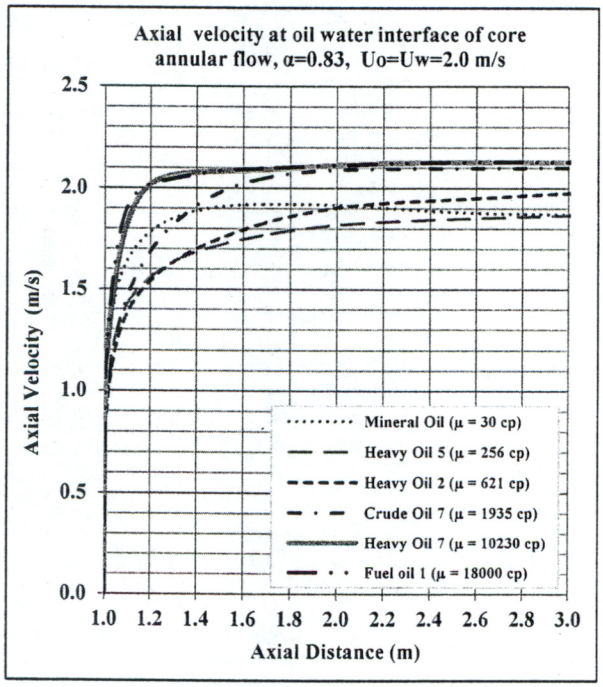

Figure (11a) Axial Velocity

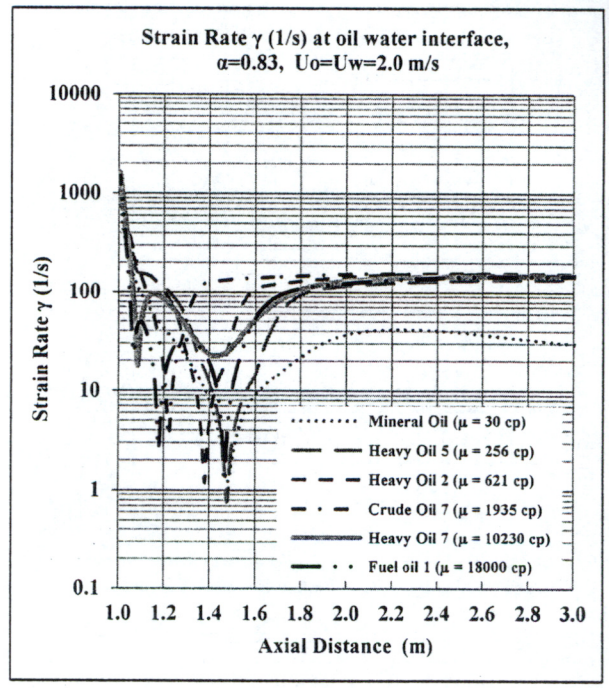

Figure (11b) Strain Rate γ

Figure (11)
Development at oil-water interface of core-annular pipe flow, α=0.83

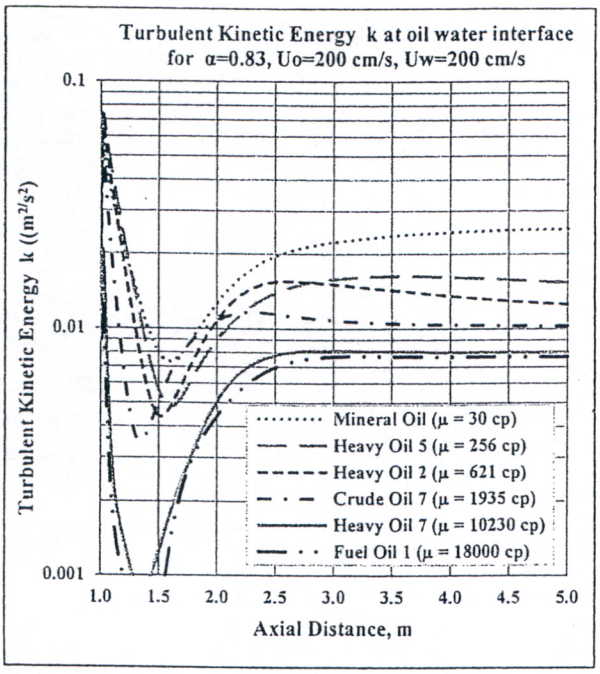

Figure (12a) Turbulent Kinetic Energy *k*

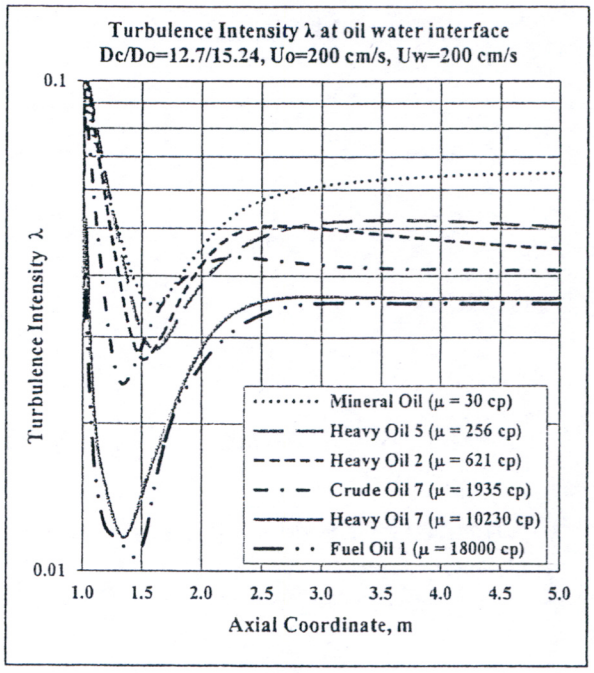

Figure (12b) Turbulence Intensity λ

Figure (12)
Development at oil-water interface of core-annular pipe flow. α=0.83,

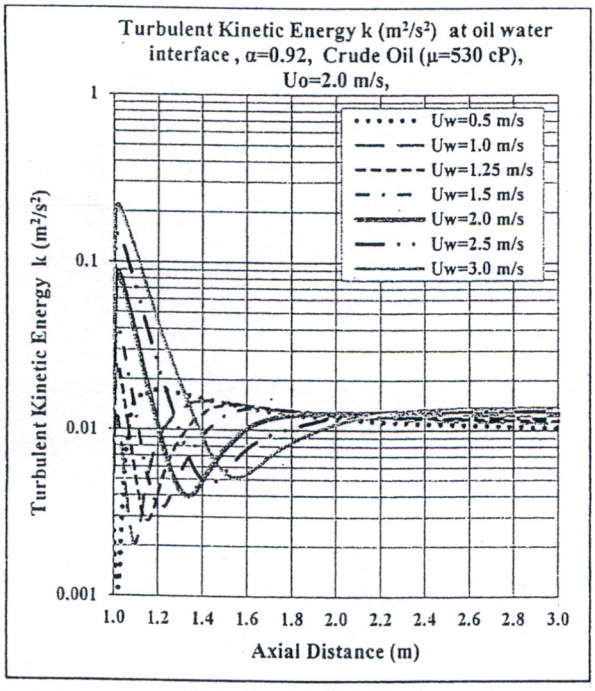

(13a) Crude Oil 1 (μ=530 cP)

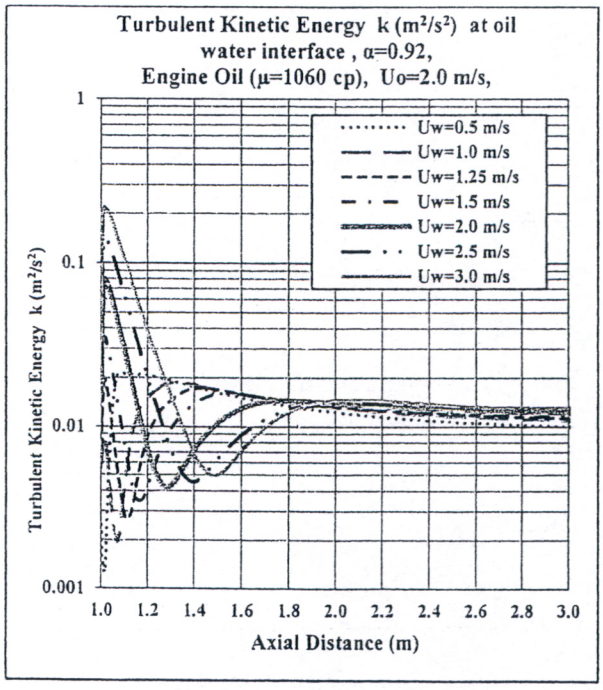

(13b) Engine Oil (μ=1060 cP)

Figure (13)
Development of Turbulent Kinetic Energy k at oil – water interface, α=0.92